Geometries, stability and dissociation behavior of Ag_nCo clusters (n = 1-12): A theoretical investigation

Nguyen Thi Mai[1,2], Ngo Thi Lan[2,3], Nguyen Thanh Tung[1,2*]

[1]Institute of Materials Science, Vietnam Academy of Science and Technology;
[2]Graduate University of Science and Technology, Vietnam Academy of Science and Technology;
[3]Institute of Science and Technology, TNU - University of Science.
[*]Email: tungnt@ims.vast.ac.vn

Received 19 Sep 2022; Revised 20 Dec 2022; Accepted 10 Apr 2023; Published 28 Apr 2023.
DOI: https://doi.org/10.54939/1859-1043.j.mst.86.2023.103-109

ABSTRACT

The geometric structure, stability, dissociation channel and magnetism of Ag_nCo clusters (n = 1–12) have been studied using density functional theory. The results show that the Co atom tends to choose the highest coordination position. The ground state of Ag_nCo clusters prefers the planar motif at small sizes (n less than 4) but favors 3D structures at larger sizes (n = 5–12). The stability of clusters is not only governed by the symmetric geometry but also strongly depends on the electronic structure and the filling rule of the electron shells. The Ag_9Co cluster with 18 valence electrons fully filled the electronic shell ($1S^21P^63d_{Co}^{10}$), which is considered as a potential superatom. The total magnetic moment of Ag_nCo clusters is governed by the electron localization on the Co atom. The relative stability of the clusters is determined by the average binding energy, the second-order difference energies, and the dissociation energies.

Keywords: Density functional theory; Silver clusters; Cobalt clusters; Dissociation energies.

1. INTRODUCTION

Recently, clusters of noble metal atoms doped with transition metal atoms have been considered as one of the hot topics in the field of materials science due to their huge potential in tailoring the chemical and physical properties of novel building blocks for advanced nanomaterials [1-6]. Among them, silver-based clusters have received a considerable attention with numerous studies by density functional theory (DFT) [7-10] and various experimental techniques thanks to their precious optical and catalytic properties [11-14]. Doping transition metal atoms in silver clusters have resulted in the desired properties for potential applications in optics, sensing, biochemistry, medicine, and nanotechnology [15-19]. For example, the widening and quenching of the peaks in the visible UV absorption spectrum of silver clusters have been observed in the Ag_n clusters doped with Si atom [15]. The optical properties of the Ag_nAu_m cluster can be changed by the ratio of the number of silver atoms to that of gold atoms, showing Au_4Ag_4 as a promising molecule for photovoltaic devices [16]. Ag-Cu alloy is considered as a potential candidate to replace the noble Pt-based catalyst in alkaline fuel cells [19]. The valence electrons in the outermost shell of the $Ag_{12}Cu$ cluster are found more active than those of the Ag_{13} cluster [20]. While Ag_{12} is estimated to be less stable, the stability of the Ag_{12} cluster is enhanced when doped with a *3d* transition metal atom [21]. Recently, silver clusters doped with vanadium have been investigated thanks to their unique physical and chemical properties [22-25]. Zhang et al. illustrated that the relative binding energy of neutral $Ag_{12}V$ cluster is larger than that of the tetrahedron Ag_{13} [22]. The stability of transition metal doped silver clusters (Ag_nTM^+ with TM = Sc, Ti, V, Cr, Mn, Fe, Co, Ni) has been found to depend on the composition and size of the silver clusters.

To our best knowledge, the geometric structure and magnetic properties of Ag_nCo clusters have been investigated at small sizes (n = 1-9) [26]. Unfortunately, the stability, dissociation energy, and electronic structure of these clusters have not been systematically reported yet. In this regard, we systematically study on cobalt-doped silver clusters Ag_nCo (n = 1-12) using DFT

calculations. The stability, dissociation energy, molecular energy level diagram, and the local/total magnetic moment will be calculated in detail in the next section.

2. COMPUTATIONAL METHOD

In this work, the structures and properties of Ag_nCo clusters were studied using density functional theory (DFT). All calculations were computed using the Gaussian software version 09 [27, 28] and the supported software, Gaussview 16. We use the BP86 functional in conjunction with cc-pVTZ-pp basis set for the Ag atom and cc-pVTZ basis set for the Co atom. Our results summarized in table 1 are in a good agreement with experimental values. The ground state structures of Ag_nCo clusters are determined as follows: Firstly, all the possible geometries of Ag_n clusters were built by Gaussview software. These structures are used as input data for the geometry optimization, which is combined with non-negative frequency vibration calculations. A Co atom was then substituted for an Ag atom in all possible positions in the most stable structures of Ag_n clusters to form the input geometrical structures of the Ag_nCo clusters. The search for energy minima structure followed by frequency was conducted using this approach. The total magnetic moments and the local magnetic moments were defined as the difference between the numbers of spin-up and spin-down electrons occupying the molecular/atomic orbitals of the clusters/atoms.

Table 1. *The bond lengths (R in Å) and dissociation energies (D_e in eV) of the ground state Ag_2 and Cr_2 dimers.*

Dimers	Functional/Basis set	R (Å)		D_e (eV)	
		Calc.	Expt.	Calc.	Expt.
Ag_2	BP86/cc-pvTZ-pp	2.56	2.53 [29]	1.62	1.63 ± 0.03 [29]
	BP86/LanL2DZ	2.48		1.60	
	B3LYP/LanL2DZ	2.45		1.58	
Co_2	BP86/cc-pvTZ	2.29	2.31 [30]	1.69	1.73 ± 0.26 [30]
	BP86/LanL2DZ	2.23		1.56	
	B3LYP/LanL2DZ	2.18		1.61	
AgCo	BP86/cc-pvTZ-pp (Ag) BP86/cc-pvTZ (Co)	2.42	2.43 [31]	1.76	1.86 [31]
	BP86/LanL2DZ	2.44		1.68	
	B3LYP/LanL2DZ	2.49		1.62	

3. RESULTS AND DISCUSSION

3.1. Optimized structures

According to the aforementioned computational procedure, a large number of possible structures and spin configurations have been considered to determine the global minima of each Ag_nCo clusters. The most stable structural optimizations and spin configurations of the Ag_nCo clusters with n = 1-12 are illustrated in figure 1, Ag_{n+1} clusters are included for comparison.

It can be seen that the ground-state Ag_nCo clusters prefers planar structures at small sizes ($n \leq 4$). In these species, the substitution of an Ag by a Co atom tends to resemble the lowest-lying structure of Ag_{n+1}. There was a structural transition from 2D to 3D occurring at n = 5. At larger sizes, the most stable structure of Ag_nCo clusters shows that the Co atoms favor occupying the highest coordination positions, maximizing the number of Ag-Co bonds. It is worth mentioning that the lowest-lying Ag_nCo clusters have a clear evolutionary rule. While the most stable structure of the Ag_nCo clusters favors the trapezoid shape for n = 1-4, the endohedral shapes are preferred at

n = 5-12. Remarkably, the ground state structure of Ag_9Co has the form of a distorted square prism C_{2v}, which is bounded by an Ag atom on top and the Co atom surrounded by Ag atoms.

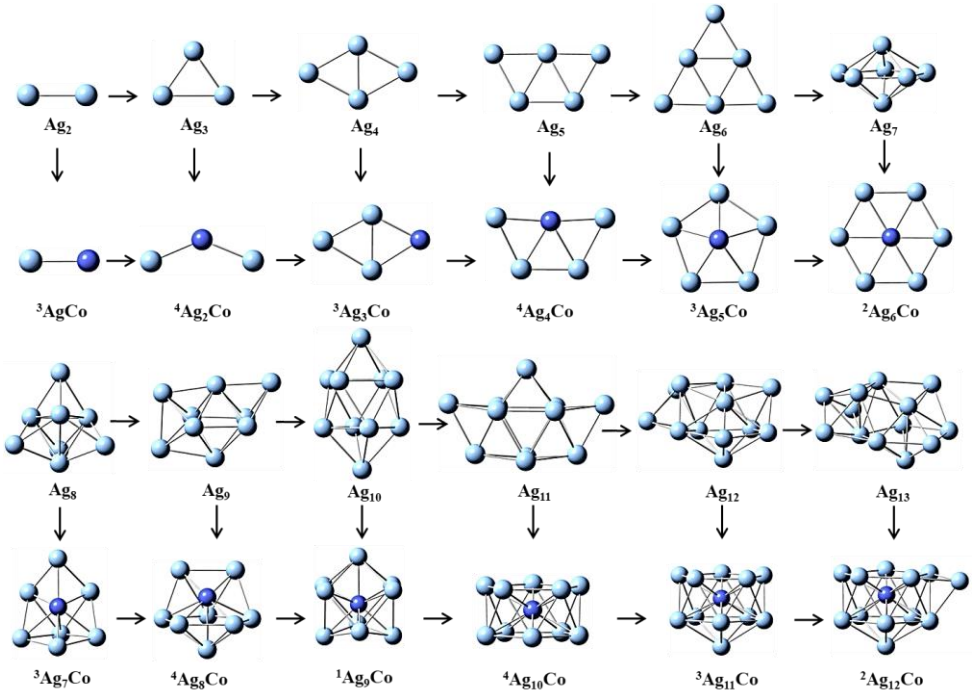

Figure 1. *The ground-state structures of pure Ag_{n+1} and doped Ag_nCo (n = 1-12) clusters. The spin multiplicity and energy difference compared to each ground-state structure are given.*

3.2. Relative stability

In order to investigate the influence of substituting an Ag atom by a Co atom on the cluster stability, we calculated their average binding energy (E_b in eV), the second-order difference energies (Δ_2E in eV). The E_b and the Δ_2E of a given cluster are a measure of its energy stability. The average binding energy of Ag_{n+1} clusters, Ag_nCo clusters, and the second-order difference energies of Ag_nCo clusters are calculated by using the following formulas:

$$E_b(Ag_{n+1}) = \frac{\left[(n+1)E_{Ag} - E_{Ag_{n+1}}\right]}{n+1} \quad (1)$$

$$E_b(Ag_nCo) = \frac{nE_{Ag} + E_{Co} - E_{Ag_nCo}}{n+1} \quad (2)$$

$$\Delta_2E(CoAg_n) = E(CoAg_{n+1}) + E(CoAg_{n-1}) - 2E(CoAg_n) \quad (3)$$

where $E_{Co}, E_{Ag}, E_{Ag_nCo}, E_{Ag_{n+1}}$ are the total electron energies of Co, Ag, Ag_nCo, and Ag_{n+1}, respectively.

The calculated E_b for the ground state structures of Ag_{n+1} and Ag_nCo clusters are illustrated in figure 2(a). The E_b values of the Ag_nCo for all sizes are generally larger than those of pure Ag_{n+1} clusters (except for n = 2). The striking stability enhancement of Co doped species can be attributed to the difference binding energies between Ag-Co and Ag-Ag. As shown in figure 2(a), the Ag-Co average binding energy (E_b = 0.89 eV) is evidently stronger than that of Ag-Ag (E_b = 0.81 eV). Thereby, substituting one Ag atom by one Co atom causes a significant change in the distribution of bonding energy and consequently a structural change of Ag_n clusters, especially at large sizes (n = 5-12). The structural motif with the Co-doped atom in the central position was determined to be the most stable for the Ag_nCo clusters since it can maximize the number of stronger AgCo bonds and enhance the cluster stability. Remarkably, with the high average

binding energy of 1.73 eV, the Ag_9Co cluster is considered to be the stable cluster. In order to confirm the stability of the doped clusters, we calculated the second-order difference energies as shown in Fig. 2(b). Compare to the other neighboring sizes, the second-order difference energies of the Ag_9Co is the largest at 1.34 eV. This result is completely consistent with the stability of the Ag_9Co cluster according to the average binding energy value (figure 2(a)).

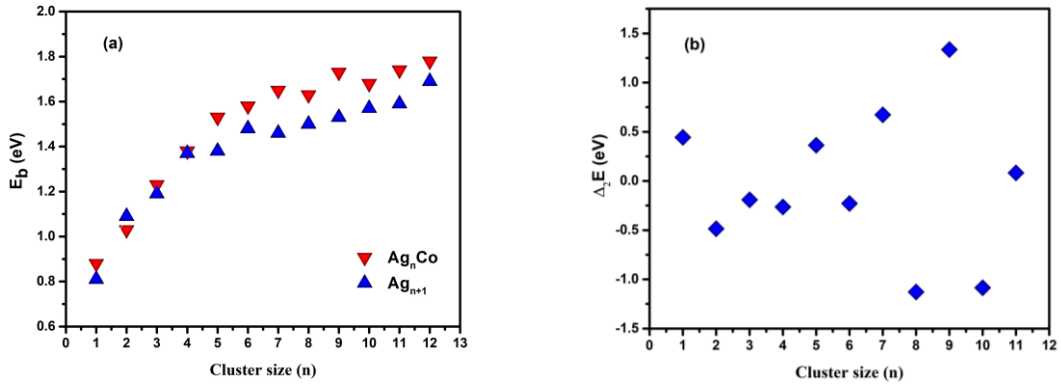

Figure 2. *(a) Average binding energies (E_b in eV) of Ag_{n+1} and Ag_nCo and (b) second-order differential energies ($\Delta_2 E$ in eV) of Ag_nCo.*

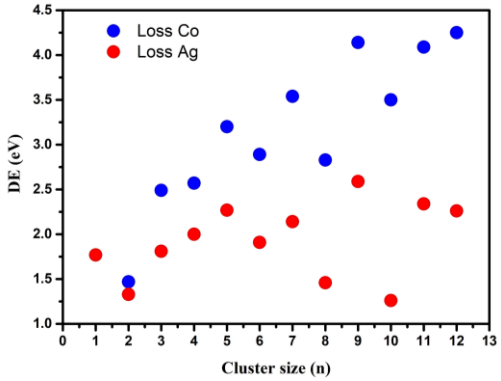

Figure 3. *Dissociation energies of Ag_nCo to evaporate one Ag or Co atom.*

In order to evaluate the thermodynamic stability of the clusters, we conducted a calculation of the dissociation energies (DEs) of Ag_nCo clusters in two possible channels: evaporating either a Co or an Ag atom. The dissociation energies are determined by using the following formulas:

$$DE\ (Co) = E(Ag_n) + E(Co) - E(Ag_nCo) \quad (4)$$

$$DE\ (Ag) = E(Ag_{n-1}Co) + E(Ag) - E(Ag_nCo) \quad (5)$$

where E represents the energy of the corresponding clusters or atoms. The dissociation energies are defined as the difference between the total electronic energies of the species formed in each dissociation channel and the electronic energies of the parent clusters. The results are shown in figure 3. Our calculations indicated that the evaporation of an Ag atom is an easier channel than that of a Co atom. It requires only 1.26 eV to evaporate one Ag atom from $Ag_{10}Co$ to form Ag_9Co cluster, suggesting that the $Ag_{10}Co$ cluster is the most fragile and confirm the tendency to form the stable Ag_9Co. Interestingly, the DE value of the Ag_9Co cluster is significantly high for both dissociation channels. The minimum energy to fragment Ag_9Co into an Ag atom and Ag_8Co cluster is 2.59 eV. This result is in an excellent agreement with the average binding energy and quadratic energy values which are discussed in the previous section.

3.3. Magnetic properties

Theoretical studies have shown that the magnetism of a cluster is governed by the structure,

size, and composition of the clusters. The total and local magnetic moments of ground-state Ag_{n+1} and Ag_nCo (n = 1-12) clusters are calculated and shown in table 2. The magnetic behavior of pure silver clusters are known with odd-even staggering feature. Compared to the pure silver Ag_{n+1} clusters, the magnetism of the dopant clusters Ag_nCo alters significantly. The total magnetic moment of the clusters with odd n is 2 μ_B except for the Ag_9Co, whose magnetic moment is completely quenched. For the ground-state Ag_nCo clusters with even n, the total magnetic moments are 3 μ_B for n = 2, 4, 8 and 10 while it is 1 μ_B for n = 6 and 12. It should be noted that the magnetic moment of doped cluster is primarily derived from the localized electrons on the 3d orbital of the Co atom. The partially filled 3d orbitals plays an important role in forming the magnetism of the Co atom. The 4s and 4p orbitals of the Co atom contribute a small amount to the magnetic moment of the Ag_nCo clusters, depending on the atomic cluster size.

Table 2. *Total magnetic moment, local magnetic moment on Ag atoms, Co atom and AO-3d, AO-4s, AO-4p of Co atom in clusters Ag_nCo (n = 1-12).*

n	Total magnetic moment	Local magnetic moment Ag atom	Local magnetic moment Co atom	Local magnetic moment		
				Co-3*d*	Co-4*s*	Co-4*p*
1	2	-0.10	2.10	2.01	0.09	0.00
2	3	0.53	2.47	2.29	0.11	0.06
3	2	-0.21	2.21	2.10	0.12	-0.02
4	3	0.57	2.43	2.14	0.18	0.11
5	2	0.04	1.96	1.89	0.04	0.04
6	1	-0.58	1.58	1.52	0.04	0.00
7	2	0.14	1.86	1.74	0.06	0.06
8	3	1.08	1.92	1.82	0.06	0.04
9	0	0.00	0.00	0.00	0.00	0.00
10	3	1.46	1.54	1.54	0.00	-0.02
11	2	1.06	0.94	0.95	0.00	-0.03
12	1	0.09	0.91	0.91	0.00	-0.01

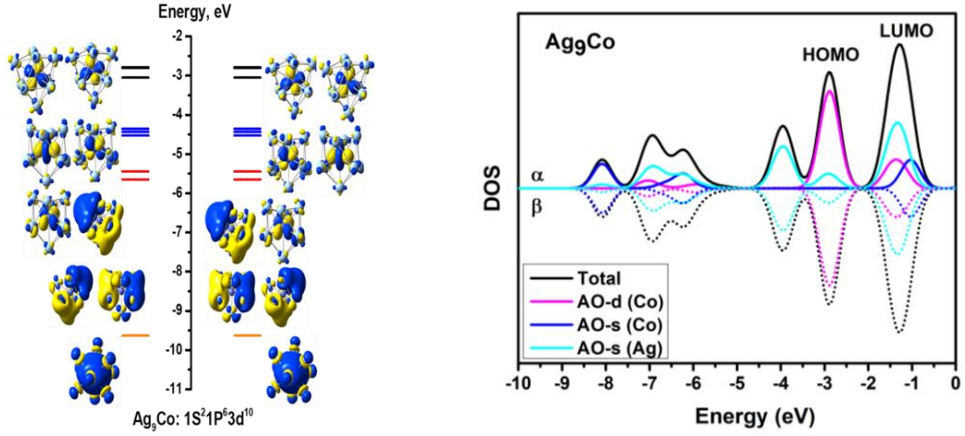

Figure 4. *Molecular orbital diagrams (MO) (right) and total/partial density of states (DOS) (left) of Ag_9Co clusters.*

The Ag_9Co cluster with the Co atom encapsulated by nine Ag atoms is an interesting case, where the total magnetic moment is completely quenched. Unlike the $Ag_{12}Cr$ and $Cu_{12}Cr$ [32] with 18 electron that correspond to the full electronic shell of $1S^21P^61D^{10}$, the Ag_9Co has an closed-electronic shell of $1S^21P^63d^{10}$ as shown in Fig. 4. This electronic configuration corresponds to a filled molecular shell ($1S^21P^6$) of 8 valence electrons and a filled atomic shell ($3d^{10}$) of 10 localized electrons. At this size, the valence electrons in the outermost shell ($3d^74s^2$)

of the Co atom seem to be strongly localized on its 3d orbitals and do not participate in the molecular shell. There is even one electron transferred from Ag atoms to 3d states of Co atom to achieve the $3d^{10}$ configuration. The shell closure of Ag_9Co with a saturated configuration of $3d_{Co}^{10}$ creates a stable electronic structure and enhance the cluster stability. As shown in figure 5, the MO and DOS diagram show the partial hybridization between 3*d*-Co and 5*s*-Ag electrons in Ag_9Co cluster. The MO diagram also confirm the formation of the filled atomic shells of 3*d*-Co electrons and that of the filled molecular shell, creating a stable electronic structure with a unique 18 electron configuration $1S^21P^63d_{Co}^{10}$.

4. CONCLUSIONS

The geometries, electronic structures, dissociation behavior, and magnetic properties of Ag_nCo (n = 1-12) clusters were investigated using DFT calculations. The lowest energy isomers for Ag_nCo ($n \leq 4$) clusters favor planar structures, whereas larger ones prefer three-dimensional motif. The calculations show that the total magnetic moment of Ag_nCo clusters is mainly localized on the Co atom. Analysis of the stability of Ag_nCo clusters shows that Ag_9Co is a cluster with highest stability compared to other sizes. The molecular orbital analysis in combination with the density of states and the shell model shows that of Ag_9Co has shell-closure configuration of $1S^21P^63d_{Co}^{10}$ and be potential as a superatom.

Acknowledgments: *This work was supported by the Vietnam Academy of Science and Technology under grant number VAST03.03/21-22.*

REFERENCES

[1]. Medel, V.M., et al., "*Nature of Valence Transition and Spin Moment in Ag_nV^+ Clusters"*, Journal of the American Chemical Society, **136**, 8229-8236, (2014).

[2]. Ngo Thi Lam., et al., "*DFT investigation of Au_9M^{2+} nanoclusters (M = Sc-Ni): The magnetic superatomic behavior of Au_9Cr^{2+}"*, Chem. Phys. Lett., 793, 139451, (2022).

[3]. A. Yang, W. Fa, J. Dong, *"Magnetic Properties of Transition Metal Doped Tubular Gold Clusters: M@Au24 (M=V, Cr, Mn, Fe, Co and Ni)"*, J. Phys. Chem. A, **114**, 4031, (2010).

[4]. F. Alkan, A. Muñoz-Castro, C.M. Aikens, *"Relativistic DFT Investigation of Electronic Structure Effects Arising from Doping the Au_{25} Nanocluster with Transition Metals"*, Nanoscale, 9, 15825, (2017).

[5]. Zhang, M., et al., "*Low-energy isomer identification, structural evolution, and magnetic properties in manganese-doped gold clusters $MnAu_n$ (n= 1–16)"*, The Journal of Physical Chemistry A, **116** 1493, (2012).

[6]. Nguyen Minh Tam, Nguyen Thi Mai, Hung Tan Pham, Ngo Tuan Cuong and Nguyen Thanh Tung, "*Ultimate Manipulation of Magnetic Moments in the Golden Tetrahedron Au_{20} with a Substitutional 3d Impurity*", J. Phys. Chem. C 122, 16256, (2018).

[7]. Hou, X.-J., et al., "*Theoretical study of the geometric and electronic structure of neutral and anionic doped silver clusters, $Ag_5X^{0,-}$ with X= Sc, Ti, V, Cr, Mn, Fe, Co, and Ni"*, Chemical physics, **330,** 379, (2006).

[8]. Dong, R., et al., "*Structural, electronic and magnetic properties of Ag_nFe clusters ($n \leqslant 15$): local magnetic moment interacting with delocalized electrons"*, Journal of Physics B: Atomic, Molecular and Optical Physics, **44**, 035102, (2011).

[9]. Harb, M., F. Rabilloud, and D. Simon, "*Structural, electronic, magnetic and optical properties of icosahedral silver–nickel nanoclusters"*, Physical Chemistry Chemical Physics, **12** 4246, (2010).

[10]. R. Xiong, D. Die, Y.G. Xu, B.X. Zheng, Y.C. Fu "*Probing the Structural, Electronic and Magnetic Properties of Ag_nSc (n=1-16) Clusters*", Phys. Chem. Chem. Phys., **20**, 15824, (2018).

[11]. Chakra P. Joshi, Megalamane S. Bootharaju, and Osman M. Bakr "*Tuning Properties in Silver Clusters*", J. Phys. Chem. Lett. **6**, 15, 3023, (2015).

[12]. Xi Kang, Yingwei Li, Manzhou Zhu and Rongchao Jin, "*Atomically precise alloy nanoclusters: syntheses, structures, and properties"*, Chem. Soc. Rev., 49, 6443, (2020).

[13]. Huayan Yang, Yu Wang, Huaqi Huang, Lars Gell, Lauri Lehtovaara, Sami Malola, Hannu Häkkinen & Nanfeng Zheng, "*All-thiol-stabilized Ag_{44} and $Au_{12}Ag_{32}$ nanoparticles with single-crystal structures*", Nature Communications 4, 2422, (2013).

[14]. Jie Yang, Runqiang Pang Dongpo Song and Man-Bo Li "*Tailoring silver nanoclusters* via *doping: advances and opportunities*", Nanoscale Adv., 3, 2411, (2021).
[15]. Mokkath, J.H. and U. Schwingenschlögl, "*Structural and optical properties of Si-doped Ag clusters"*, The Journal of Physical Chemistry C, **118**, 4885, (2014).
[16]. Zhao, G.-f., J.-m. Sun, and Z. Zeng, "*Absorption spectra and electronic structures of Au_mAg_n (m+ n= 8) clusters".* Chemical Physics, **342**, 267, (2007).
[17]. Li, W. and F. Chen, "*Alloying effect on performances of bimetallic Ag–Au cluster sensitized solar cells"*, Journal of Alloys and Compounds, **632**, 845, (2015).
[18]. Chang, L., H. Xu, and D. Cheng, "*Role of ligand type on the geometric and electronic properties of Ag–Au bimetallic clusters".* Computational and Theoretical Chemistry, **1045**, 35, (2014).
[19]. Zhang, N., F. Chen, and X. Wu, "*Global optimization and oxygen dissociation on polyicosahedral Ag32Cu6 core-shell cluster for alkaline fuel cells"*, Scientific reports, **5**, 1, (2015).
[20]. Ma, W. and F. Chen, "*Optical and electronic properties of Cu doped Ag clusters"*, Journal of alloys and compounds, **541**, 79, (2012).
[21]. Sargolzaei, M., N. Lotfizadeh, "*Spin and orbital magnetism of a single 3 d transition-metal atom doped into icosahedral coinage-metal clusters X_{12} (X= Cu, Ag, Au)"*, Physical Review B, **83**, 155404, (2011).
[22]. Zhang, M., et al., "*Probing the magnetic and structural properties of the 3d, 4d, 5d impurities encapsulated in an icosahedral Ag_{12} cage"*, Physica B: Condensed Matter, **405**, 642, (2010).
[23]. Chen, L., et al., "*Chemical coupling sers properties of pyridine on silver-caged metal clusters M@ Ag_{12} ($M= V^-, Nb^-, Ta^-, Cr, Mo, W, Mn^+, Tc^+, Re^+$)"*, Journal of Electronic Materials, **46**, 3904, (2017).
[24]. Medel, V.M., et al., *Nature of valence transition and spin moment in Ag_nV^+ clusters.* Journal of the American Chemical Society, **136**, 8229, (2014).
[25]. Gong, X., et al., "*Spin–orbit Splitting and Magnetism of Icosahedral M@ Ag_{12} Clusters (M= 3d and 4d atoms)"*, Journal of Cluster Science, **26**, 759, (2015).
[26]. Rodríguez-Kessler, P.L. and A.R. Rodríguez-Domínguez, "*Structural, electronic, and magnetic properties of Ag_nCo (n=1–9) clusters: A first-principles study"*, Computational and Theoretical Chemistry, **1066**, 55, (2015).
[27]. Frisch, M., et al., "*Gaussian 09, revision D. 01*. 2009", Gaussian, Inc., Wallingford CT, (2009).
[28]. Hohenberg, P. and W. Kohn, "*Density functional theory (DFT)"*, Phys. Rev, **136**, B864 (1964).
[29]. Simard, B., et al., "*The bond length of silver dimer"*, Chemical physics letters, **186**, 415, (1991).
[30]. Kant, A. and B. Strauss, "*Dissociation energies of diatomic molecules of the transition elements. II. Titanium, chromium, manganese, and cobalt"*, The Journal of Chemical Physics, **41**, 3806, (1964).
[31]. Li, S.F., et al., "*Role of Ag-doping in small transition metal clusters from first-principles simulations"*, The Journal of Chemical Physics, **131,** 184301, (2009).
[32]. Mai, N.T., et al., *Systematic Investigation of the Structure, Stability, and Spin Magnetic Moment of CrM_n Clusters (M = Cu, Ag, Au, and n = 2–20) by DFT Calculations"*, ACS Omega, **6**, 20341, (2021).

TÓM TẮT

Cấu trúc, độ ổn định và quá trình phân ly của cụm nguyên tử Ag_nCo (n=1-12): Một nghiên cứu lý thuyết

Cấu trúc hình học, độ ổn định, năng lượng phân ly và từ tính của các cụm nguyên tử Ag_nCo (n = 1–12) đã được nghiên cứu bằng cách sử dụng lý thuyết hàm mật độ. Kết quả cho thấy nguyên tử Co có xu hướng lựa chọn vị trí có số phối trí cao nhất. Các cụm nguyên tử Ag_nCo có dạng hình học phẳng ở kích thước nhỏ (n = 4) và tạo thành cấu trúc 3D ở kích thước lớn hơn (n = 5–12). Tính bền vững của các cụm nguyên tử không chỉ bị chi phối bởi cấu trúc hình học mà còn phụ thuộc mạnh vào cấu trúc điện tử. Đặc biệt, cụm Ag_9Co với 18 điện tử hóa trị lấp đầy lớp vỏ điện tử ($1S^21P^63d_{Co}^{10}$), được tiên đoán là một siêu nguyên tử tiềm năng. Điều thú vị là tổng mômen từ của các cụm Ag_nCo phụ thuộc vào các điện tử định xứ trên nguyên tử Co. Tính bền vững tương đối của các cụm được xác định bởi năng lượng liên kết trung bình, sự chênh lệch năng lượng liên kết bậc hai và năng lượng phân ly.

Từ khóa: Phiếm hàm mật độ; Cụm nguyên tử bạc; Cụm nguyên tử cobalt; Quá trình phân ly.